JOC The Journal of Organic Chemistry

Article

pubs.acs.org/joc

Electronic Structural Trends in Divalent Carbon Compounds

Han Vinh Huynh[†] and Gilles Frison*[,‡]

[†]Department of Chemistry, 3 Science Drive 3, National University of Singapore, Singapore 117543

[‡]Laboratoire des Mécanismes Réactionnels, Department of Chemistry, Ecole Polytechnique and CNRS, 91128 Palaiseau Cedex, France

Supporting Information

ABSTRACT: This work aims to analyze and compare the intrinsic electronic densities in a series of neutral and anionic divalent carbon-donor derivatives. The σ-lone pair at the divalent carbon is the HOMO of these species. Structural factors have been identified that influence its energy, which is a measure of the σ-basicity. The π-electronic structure has been described as a function of the π-population. Our results show that no straightforward structural criteria correlate with the π-electronic distribution. However, the π-population, as well as the π-acidity and π-basicity, are related to the π-MOs. In all cases, these π-MOs can be qualitatively obtained on the basis of those of the protonated analogues by simply increasing the energy of the p_π orbital at the divalent carbon atom compared to normal sp^2 carbon. Such an analysis allows a rationalization of the trends observed for the π-electronic structure of these ligands. Notably, this explains the values of the π-population at the divalent carbon center, which shows an increasing and continuous range from classical NHCs to mesoionic "carbenes".

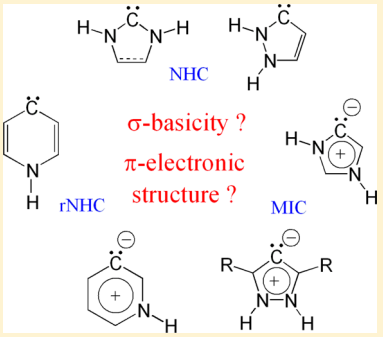

INTRODUCTION

Since their first synthesis by Bertrand[1−3] and Arduengo's[4] groups, stable singlet carbenes[5] have become very widely used in organometallic[6−8] and heteroatom chemistry[9−14] as well as in transition-metal-mediated catalysis[15−19] and organocatalysis.[20−23] Their characteristically strong electron-donating ability[24−27] makes them good nucleophiles and good ligands for numerous important processes, which include [2 + 1] cycloadditions,[28] olefin metathesis,[29] or cross-coupling reactions.[30] The versatility of classical *N*-heterocyclic carbenes (NHCs) in these areas has led to a significant amount of work dealing with their structural modification, and this has led to the discovery of a great variety of novel divalent carbon ligands that are usually included under the "carbene" umbrella. The parent structures of selected representatives **C**-**H** are presented in Scheme 1 along with their classical NHC counterparts **A** and **B**.

Scheme 1. Representative Examples of Divalent Carbon-Donor Molecules

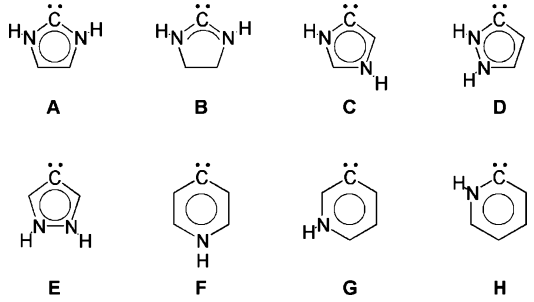

The carbene carbon atom in conventional NHCs **A** and **B** is flanked by two σ-accepting and π-donating nitrogen atoms that give rise to a significant stabilization of the singlet ground state.[5] In structures **C**-**H**, the divalent carbon atom is less well stabilized through π-donation from the heteroatom(s) (Scheme 1),[31] and compounds that do not have heteroatoms lying α- to the carbene carbon, often termed *remote* NHCs (*r*NHC),[32] are usually better donors due to lower negative inductive ($-I$) effects.[33] Despite their widespread use, it is noteworthy that the nomenclature of some of these compounds is not particularly enlightening because of ambiguities in the description of their electronic structures; for example, no clear boundaries exist between the classes of carbon(II) carbenes, carbon(0) complexes,[34,35] and ylidic compounds.[36−42] So as to eliminate any notational bias in the way we present these molecules from the outset, we draw them all with π-electron delocalization in Scheme 1, even though localized resonance structures are usually favored by the chemical community, for example, for **A** and **B**. Another potential distinction between these divalent carbon-donor molecules reflects their ability to accommodate a nonzwitterionic resonance structure. Compounds requiring the introduction of formal charges on some atoms are termed mesoionic (or abnormal) carbenes (MICs)[43,44] (**C**, **E**, and **G** in Scheme 1), and numerous representations have been proposed in the literature, as illustrated for species **E** (Scheme 2).[45−48]

Among these resonance forms, a cyclic "bent allene" resonance **E9** that has been used to describe 3,5-bis-(dialkylamino)- or 3,5-bis(aryloxy)-substituted derivatives of **E** (see **4** and **5** in Scheme 3) has been the subject of intensive

Received: October 2, 2012
Published: December 19, 2012

Scheme 2. Proposed Delocalized or Resonance Structures for Type E Structures

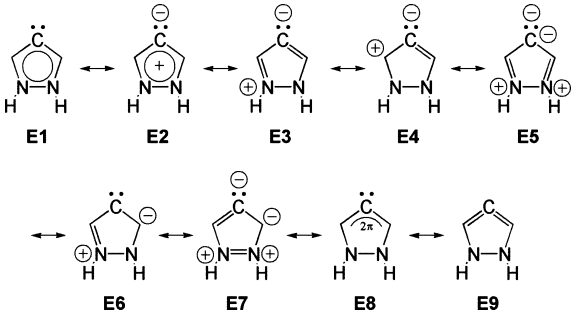

debate.[26,49−51] The electronic structure of these intriguing ligands has been the subject of thorough theoretical studies,[48,52] which show that it is difficult to describe them in terms of a unique (or predominant) resonance form. Further areas that might benefit from being addressed in more depth include how the π-electronic distribution in derivatives of **E** is modified by their 3,5-substituents (from **2** to **4** and **5**) and how ring-aromaticity is disrupted through π-delocalization of the lone pair of exocyclic nitrogen atoms in **5**. More generally, although convincing electronic descriptions are available for individual compounds from theoretical studies and there is an increasing understanding of their physicochemical properties,[27,53−57] important unanswered questions remain concerning the interpretation of differences in the electronic structures among members of the divalent carbon compound family. The σ-basicity of these compounds, which results from the lone pair located at the C_d divalent carbon, has been treated in terms of the number of adjacent nitrogen atoms,[58] but the effects of the structure of the carbene upon π-acidity and π-basicity have attracted less interest[59] and trends have not been rationalized so far. More fundamentally, it is not even clear if the distinction between "normal" and mesoionic structures, which essentially translates conventions in the way that chemical compounds are drawn, has any real meaning in terms of electronic structure.

A vast body of work aimed at better understanding the bonding of NHC and related compounds toward transition-metal complexes[60−87] has already appeared. However, in the work presented here, we focus on the intrinsic electronic structure of divalent carbon-donor molecules. Our goal is not only to provide new insight into their electronic structure but also to develop simple schemes for rationalizing electronic trends within this family. Using theoretical methods, we will examine the neutral free ligands **1**−**17**, which include species related to the experimentally known types **A**−**G** as well as model compounds designed in silico (Scheme 3). For comparison, we also include three related anionic derivatives **18**−**20** as preliminary models for strong σ-donor η^1-carbon ligands.[88−93]

RESULTS AND DISCUSSION

Optimized Geometries of 1−20 and 1(H$^+$)−20(H$^+$). The geometries of divalent carbon-donor molecules **1**−**20** in their singlet state have been optimized at the B3LYP/aug-cc-pVTZ level and are depicted in the Supporting Information (Figure S1). These structures deserve no special comment and show planar (**1**, **2**, **6**−**8**, **10**−**12**, **14**−**19**) or almost planar (**3**−**5**, **9**, **13**, **20**) arrangements around C_d. The largest deviation is obtained for **9** which has an H−N−C_d-C dihedral angle of 172.5°.

Protonation at the divalent carbon atom C_d leads to compounds **1**(H$^+$)−**20**(H$^+$), whose optimized structures are also depicted (Figure S2, Supporting Information). In all cases, this process is associated with a widening of the X−C_d−Y (X, Y = C or N) bond angle and an increasing planarization of the molecule. Both **1**(H$^+$) and **6**(H$^+$) are obtained as planar minima on the PES in the absence of any constraints during the optimization process. **9**(H$^+$), **13**(H$^+$), and **20**(H$^+$) are also planar, in contrast to their deprotonated parent derivatives **9**, **13**, and **20**, and **3**(H$^+$)−**5**(H$^+$) are found to be less distorted from planarity than **3**−**5**. These changes can be rationalized in terms of a larger p_π−p_π resonance in the protonated species than in the corresponding neutral (or anionic) carbon-donor molecules, as has already been noted for **2**, **4** and **5**,[52] **9**,[94] and **10**−**13**.[95] Addition of the proton to the anionic "dicarbene" **18** can potentially occur at the "normal" carbene center, leading to **18**^{n}(H$^+$) = **14**, or at the "abnormal" carbene center, to give **18**^{a}(H$^+$) = **11**.

σ-Basicity of 1−20. The examination of the Kohn−Sham molecular orbitals of **1**−**20** indicates that, for every case except **18**, the highest occupied molecular orbital (HOMO) describes the carbon σ-lone pair (σ-LP) which lies in the X−C_d−X plane. For **18**, the HOMO results from an antibonding combination of the two lone pairs located at each carbene center, with the

Scheme 3. Neutral (1−17) and Anionic (18−20) Divalent Carbon-Donor Molecules Studied in This Work

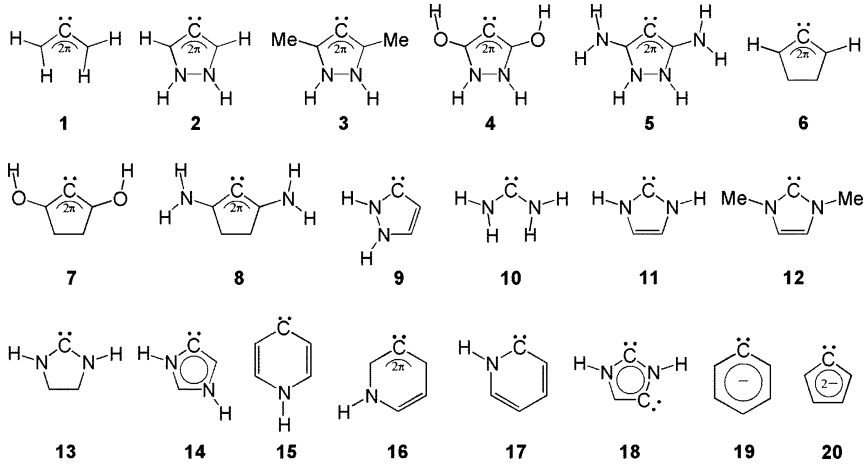

dx.doi.org/10.1021/jo302080c | J. Org. Chem. 2013, 78, 328−338

larger contribution arising from the "abnormal" carbene atom (Figure 1).

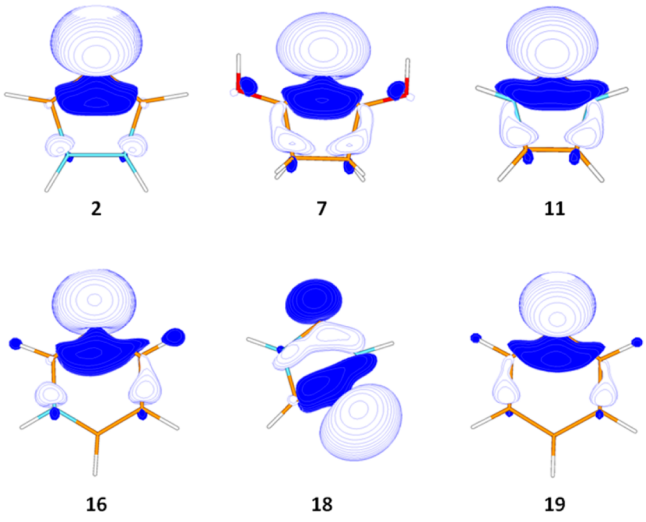

Figure 1. HOMO of some representative divalent carbon-donor molecules. Atom color code: orange, carbon; light blue, nitrogen; red, oxygen; white, hydrogen.

Frenking and co-workers have demonstrated that a strong correlation exists between the proton affinity (PA) at the carbon donor and the eigenvalues of the σ lone-pair orbitals $\varepsilon(\sigma\text{-LP})$ for divalent carbon(0) compounds and type **A** and **C** carbenes.[96,97] Figure 2 shows that this correlation can be

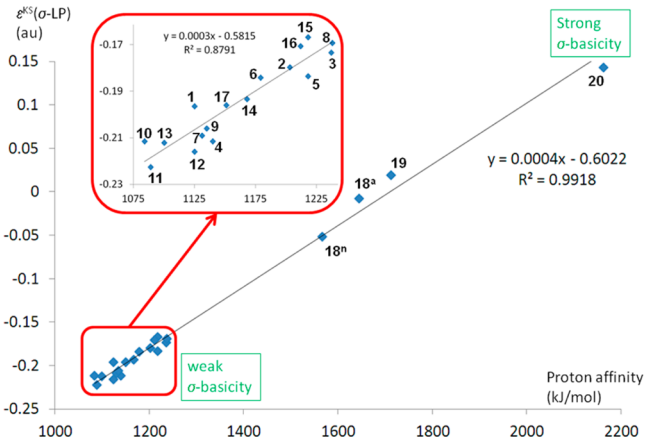

Figure 2. Plot of calculated B3LYP/aug-cc-pVTZ proton affinity versus the Kohn–Sham eigenvalues of the σ-lone pair located at the C_d carbon atom (which corresponds to the HOMO, except for $\mathbf{18^n}$ where it is HOMO-2) for compounds **1**–**20**.

extended, with an even better correlation coefficient (R^2) of 0.992, to a larger variety of 5- or 6-membered cyclic backbone structures, as well as to neutral and anionic species. The explanation of the poorer coorelation when restricting the comparison to neutral divalent carbon-donor molecules **1**–**17** (R^2 = 0.879) probably lies in the energy that is associated with the geometry change upon protonation, which forms part of the calculated PA.[96] This energy change is insignificant over a large PA range, but energies associated with the change in geometry can become non-negligible with respect to PA when changes in PA are small. This explains the lower agreement.

The correlation given above provides a clear σ-basicity scale for divalent carbon compounds, which as noted previously,[64] can be extrapolated to predict their σ-donor strength when they are employed as ligands. Analyzing the positions of **1**-**20** on this PA-derived scale reveals several factors that affect their characteristics. Overall, the charge of the divalent carbon-donor molecule makes the most important contribution to the σ-basicity of the ligand. Then, for any given charge, the calculations confirm that the identity of the atoms lying α- with respect to C_d is the dominant influence. The higher electronegativity of nitrogen versus carbon means that derivatives having an N–C_d–N moiety (**10**–**13** for neutral cases; $\mathbf{18^n}$ for an anionic case) have lower σ-donor strength than those presenting an N–C_d–C structure (**9**, **14** and **17** for neutral cases; $\mathbf{18^a}$ for an anionic case), and in turn, these are less aggressively donating than C–C_d–C moieties (**2**, **3**, **5**, **8**, **15**, and **16** for neutral cases; **19** for an anionic case). Atoms in the β-position relative to C_d also appear to play a notable role. Thus, the presence of highly electronegative oxygen atoms means that **4** and **7** are weaker σ-donors than **5** and **8**, respectively.[46] Consistently, **11** is a weaker σ-donor than **13** because the sp^2-hybridized carbon atom has a lower electronegativity than the sp^3-hybridized one,[98] as has been confirmed experimentally by ^{13}C NMR spectroscopy.[99]

Compounds **1** and **6** do not fit into this picture because their σ-basicity is computed to be significantly lower than that of **2**. It is clear that the wider CC_dC bond angle found in **1** than **2** is not the cause of this effect. Calculations upon $\mathbf{1^a}$ and $\mathbf{1^a(H^+)}$, which are analogues of **1** and $\mathbf{1(H^+)}$ wherein the CC_dC bond angles are constrained to the values observed in **2** (101.0°) and $\mathbf{2(H^+)}$ (106.1°), respectively, show that the proton affinity of $\mathbf{1^a}$ (1109 kJ/mol) is smaller than that of **1** (1125 kJ/mol) and thus also of **2** (1203 kJ/mol). This is to be expected, given the more negative eigenvalue of the σ-LP (−0.249 and −0.231 au in $\mathbf{1^a}$ and **1**, respectively) that translates the higher lone pair s character (hybridization of $sp^{1.39}$ and $sp^{1.62}$, respectively). On the other hand, examination of the HOMOs in Figure 1 suggests that the localized σ-lone pair could be stabilized by a two-electron interaction with the antibonding orbital of the X_α–Y_β bond (X_α, Y_β = H, C, or N in α and β position relative to C_d) that lies *trans* to the σ-LP (i.e., the endocyclic bond for cyclic compounds), which we will note as *trans*-$\sigma^*(X_\alpha\text{-}Y_\beta)$. NBO calculations of the second-order perturbation energy confirm that the larger contribution associated with σ-LP comes from *trans*-$\sigma^*(X_\alpha–Y_\beta)$. Electronegativity differences give the order $\varepsilon(\sigma^*(CH)) < \varepsilon(\sigma^*(CC)) < \varepsilon(\sigma^*(CN))$, which may explain why the σ-lone pair in **1** and **6** is more stabilized, and therefore less available for σ-donation, than in **2**. The role of the *trans*-$\sigma^*(X_\alpha–Y_\beta)$ can be related to the effect of the ring size on the σ-donor strength of *N*-heterocyclic carbenes.[27,100–103] Indeed, extending the NHC from a 5- to a 6- or 7-membered ring decreases the stabilizing overlap between the σ-LP and *trans*-$\sigma^*(X_\alpha–Y_\beta)$, thus enhancing the σ-donor strength. This is in agreement with experimental results.

π-Electronic Population of 1–20. The π-electronic structure of **1**–**20** is not straightforward to address because they show several delocalized π-MO's. We choose here to use the π-electronic population at C_d as a parameter for describing the π-system. According to IUPAC, carbenes are defined as compounds containing a divalent carbon atom that bears two nonbonding electrons, and in the singlet state, these nonbonding electrons are spin-paired and located in the σ-LP. The p_π population at C_d might therefore be expected to be close to

dx.doi.org/10.1021/jo302080c | J. Org. Chem. 2013, 78, 328–338

zero. The population of the p_π orbital at C_d can be established through an NPA/DFT analysis, and Figures S3 and S4 (Supporting Information) give the atomic π-population of **1**−**20** and **1**(H^+)−**20**(H^+), respectively. Figure 3 gives a comparison between the π-population at C_d for compounds **1**−**20** and the π-population of the corresponding carbon center in **1**(H^+)−**20**(H^+).

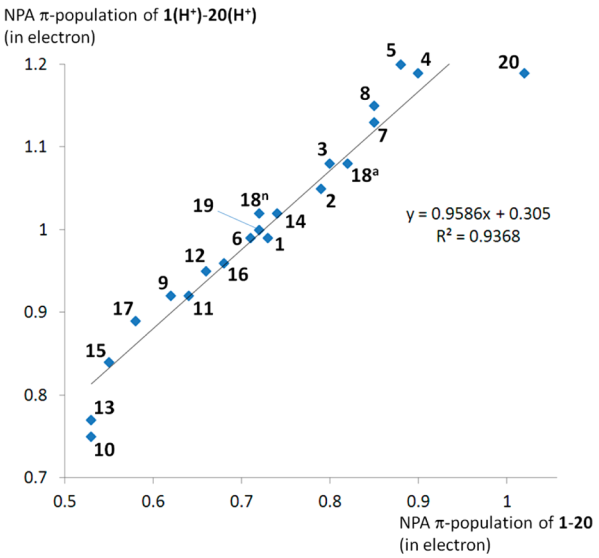

Figure 3. Plot of calculated NPA π-population at C_d in compounds **1**−**20** versus NPA π-population at the same carbon atom in **1**(H^+)−**20**(H^+).

First, we notice a relatively large range of π-population at C_d for the neutral compounds **1**−**17**, from 0.53 π-electrons in **10** and **13** to 0.90 π-electrons in **4**. Our calculations, which show that the well-known NHCs **11**−**13** have significantly more than two electrons in the σ-LP and p_π orbitals, are in accord with a previous study on **11** and **13** that gave a population of 2.46 and 2.31 nonbonding electrons for the respective at C_d atoms.[104] Even so, they have the lowest number of nonbonding electrons among the stable singlet divalent carbon compounds that we have examined. At the other end of the scale, compounds **4** and **5** have close to three electrons in the σ-LP and p_π orbitals, which indicates that these compounds are more properly described as dipolar compounds that have a negative charge at C_d than as neutral "carbenes".[105] There appears to be no clear separation between the two limiting NHC and dipolar descriptions because the compounds that we have modeled show values right across the scale. Compound **16** has a π-population of 0.68 electrons and appears approximately in the middle of the range. Previous studies have shown that **16** is best represented as a dipolar compound[36−39] so, with deference to this description, our scale implies that only **9**−**13**, **15**, and **17** should be described formally as carbenes; the MIC structures **1**−**8**, **14**, and **16** are better described as having a negative charge at C_d. The values for the NPA π-population at the C_d center in **19** and at the "abnormal" and "normal" sites in **18** indicate that the divalent carbon atoms in anionic compounds are electronically quite similar to those in mesoionic compounds. The C_d site in **20** shows an even larger π-population, which indicates that a resonance structure having a dianionic center may also be appropriate.

The NPA atomic charges at C_d (Figure S3, Supporting Information) are consistent with the above description, but the correlation is complicated by the combined effects of both the σ- and π-electronic populations. The electronic structures depicted in Scheme 2 describe changes in the π-system only and neglect polarization within the σ-bonds, which means that the formal Lewis charges are very different from the calculated NPA atomic partial charges. The electronegativity differences between C, N, and O centers, which induce the polarization of C−N and C−O σ-bonds, make a significant contribution: despite its π-population of 0.53 electrons, the C_d center in **13** has a positive NPA charge (+0.17) because it is bound to two nitrogen atoms. Conversely, the C_d center in **15**, which shows a similar π-population (0.55 electrons), has a negative NPA charge (−0.19) because its σ-bonds are not strongly polarized. Once the nature of the neighboring atoms is taken into account, it is then possible to see a relationship between the π-population and NPA charge at C_d (Figure S5, Supporting Information). Carbenes **9**−**13**, **15**, and **17** show therefore a more positive charge at C_d than their related mesoionic structures.

In depth examination of the π-population and atomic charges in **1**−**20** and **1**(H^+)−**20**(H^+) (Figures S3 and S4, Supporting Information) reveals that the distinction between carbenes and mesoionic structures in **1**−**20** that was made above has a clear parallel in **1**(H^+)−**20**(H^+), as is illustrated by the correlation (R^2 = 0.937) observed between the π-population at C_d in **1**−**20** and at the corresponding carbon center after protonation (Figure 3). This shows the limitation of drawing fine molecular description through Lewis structures. Note, for example, that while chemists are used to draw **2**(H^+), **11**(H^+), and **15**(H^+) similarly, as aromatic structures with a delocalized cationic charge, there are significant differences in the π-electronic distribution in each of these rings and between these molecules. It seems therefore difficult to define a way of describing **1**−**20** that will reflect both their differences and relationships with their protonated analogues. A dipolar description is therefore recommended for **1**−**8**, **14**, and **16** that differentiates them from "neutral" carbenes **9**−**13**, **15**, and **17**, even if there is a continuum of electronic structure between the two extremes. This dipolar description should include a cationic charge delocalized into the other atoms of the ring (and the exocyclic substituents for **3**−**5**, **7**, and **8**), as in resonance structures similar to **E3** and **E4** or, in short, to **E2** (Scheme 2).

π-Basicity of 1−20. Counterintuitively, the π-electron population is not a good parameter for evaluating the π-basicity of **1**−**20** and their protonated analogues. This is clear from the relatively poor correlation that is found between the π-population and the second PA (Figure S6, Supporting Information), which pertains to double protonation of **1**−**20** at the C_d center (Scheme S1, Supporting Information). It follows that the form of the occupied π-MOs (i.e., the weight of the p_π atomic orbital in the occupied π-MOs) that gives the π-population is not a direct measure of π-basicity.

However, as with the results obtained for divalent carbon(0) derivatives and type **A** and **C** carbenes,[96,97] the second PA value of **1**−**20** correlates with the eigenvalues of the π-HOMO[106] {ε(π-HOMO)} of the protonated derivatives **1**(H^+)−**20**(H^+) (R^2 = 0.927; Figure S6, Supporting Information). Nonetheless, it should be noted that restraining the study to the neutral species **1**−**17** almost completely nullifies the correlation (R^2 = 0.552; Figure S6, Supporting Information). The conclusion seems to be that the correlation between the second PA and the

dx.doi.org/10.1021/jo302080c | J. Org. Chem. 2013, 78, 328−338

$\varepsilon(\pi\text{-HOMO})$ of the protonated derivatives is good for carbon(0) center molecules but is not pertinent for the neutral π-delocalized systems that are under consideration here.

This result is not surprising in that the same protonated species can arise from different divalent carbon compounds. For example, while protonated forms $\mathbf{2}(\mathbf{H}^+)$ and $\mathbf{9}(\mathbf{H}^+)$ are identical, **2** and **9** do not have the same second PA (254 and 160 kJ/mol, respectively, Table S1, Supporting Information) because the protonated species result from the addition of the protons at different carbon centers (C4 in **2** versus C3 in **9**, respectively, Scheme S1, Supporting Information).

In order to better understand these absences of correlation, and therefore to give some insight in the absolute and relative π-basicities of **1**−**20**, it seems helpful to analyze their π-MOs in term of both their form and energy.

π-Molecular Orbitals. Because they constitute the simplest building blocks of most of the compounds studied here, **1** and **10** are useful as models. The parent allyl cation $\mathbf{1}(\mathbf{H}^+)$ is planar and has two delocalized π-electrons, while $\mathbf{10}(\mathbf{H}^+)$ is a 1,3-diaza-allyl cation (i.e., parent formamidinium cation) and has four delocalized π-electrons.

Their π-MOs, which are presented using Hückel calculations for clarity (Scheme 4), are quite similar in form. However, the

Scheme 4. Hückel Molecular Orbital Diagram of $\mathbf{1}(\mathbf{H}^+)$ and $\mathbf{10}(\mathbf{H}^+)$[a]

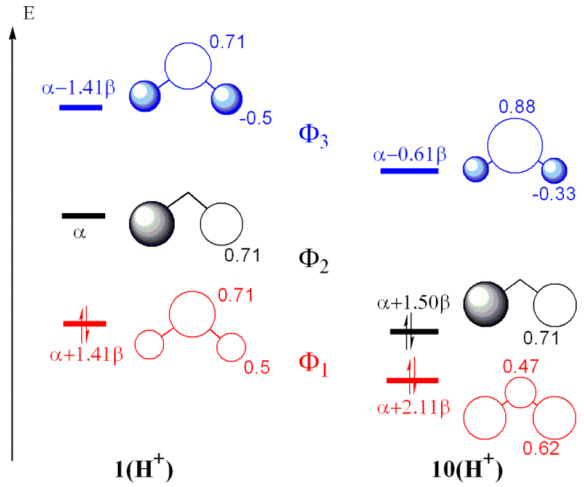

[a]The p_π orbitals are viewed from the top and represented as circles.

different number of π-electrons means that their role is very different: Φ_2 is the π-LUMO of $\mathbf{1}(\mathbf{H}^+)$ and the π-HOMO of $\mathbf{10}(\mathbf{H}^+)$. Further, the high electronegativity of nitrogen relative to carbon means that the p_π atomic orbital in the first occupied π-MO Φ_1 has a lower coefficient at the central carbon in $\mathbf{10}(\mathbf{H}^+)$ than in $\mathbf{1}(\mathbf{H}^+)$. This qualitative prediction of a lesser π-population at the central carbon of $\mathbf{10}(\mathbf{H}^+)$ than of $\mathbf{1}(\mathbf{H}^+)$ is in nice agreement with the DFT-computed π-population given above (Table S1, Supporting Information).

Comparing the MOs of the divalent carbon compounds **1** and **10** with their protonated analogues $\mathbf{1}(\mathbf{H}^+)$ and $\mathbf{10}(\mathbf{H}^+)$ reveals strong similarities. The form of the LUMO and the highest lying occupied π-orbital (i.e., the HOMO-1 of **1** and the HOMO of $\mathbf{1}(\mathbf{H}^+)$) computed at the DFT level are the same (Figure 4), which means that the π-system of **1** can be interpreted as an allylic moiety having two delocalized π-electrons. Quantitatively, **1** has only 0.73 π-electrons at C_d,

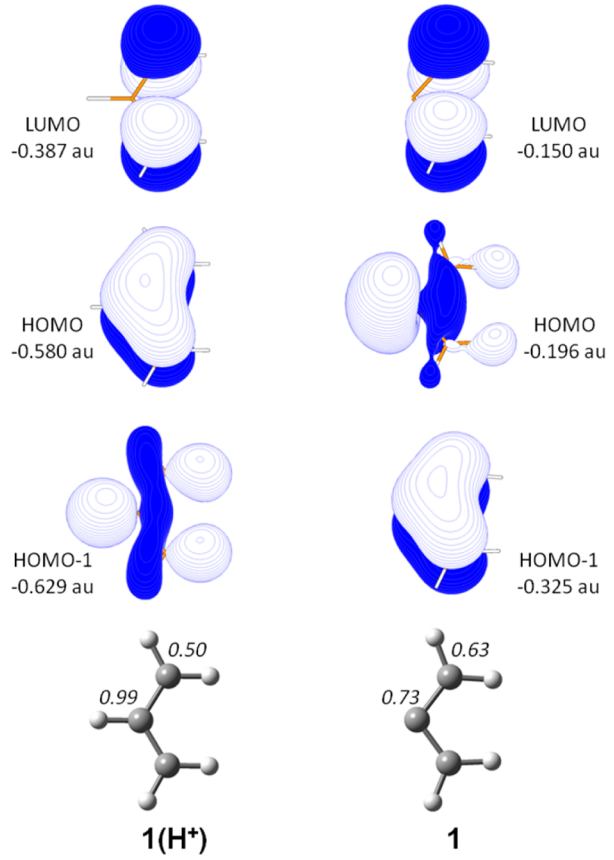

Figure 4. π-Electron population from NPA in $\mathbf{1}(\mathbf{H}^+)$ and **1** (bottom) and their HOMO-1, HOMO, and LUMO (top) computed at the B3LYP/aug-cc-pVTZ level.

which means that its HOMO-1 is less well localized on this atom than is the HOMO of $\mathbf{1}(\mathbf{H}^+)$ (Figure 4). Several explanations for this reduction in π-delocalization at C_d upon deprotonation can be proposed, which include the following: (i) the electric field induced by the proton will influence the orbital of **1** through electronic and Coulombic interactions, which will increase π-delocalization at the protonation carbon center; (ii) the σ-symmetric lone pair at C_d, the HOMO in **1**, appears to be larger than the corresponding σ_{CH} orbital (HOMO-1 in $\mathbf{1}(\mathbf{H}^+)$), so that its greater spatial extension will induce the smaller CCC bond angle in **1**.[107] It is also possible that this larger spatial extension inhibits π-delocalization at C_d. Qualitatively, we propose that the changes in the π-system that occur upon deprotonation can be viewed as a manifestation of decreasing electronegativity at the carbon atom C_d. The lower electronegativity of 0-π-electron carbon atom (i.e., C_d) compared to 1-π-electron carbon (i.e., a "normal" sp^2 carbon) then parallels the well-known decrease of the electronegativity from 2-π-electrons to 1-π-electron oxygen and nitrogen atoms in the Hückel formalism.[108,109]

The above considerations provide a simple guide to qualitatively build and analyze the π-MOs of **1**-**20** and $\mathbf{1}(\mathbf{H}^+)$−$\mathbf{20}(\mathbf{H}^+)$. Indeed, molecular orbital diagrams can be constructed for divalent carbon compounds under study by combining the π-MOs of **1** or **10** with those of small fragments like $-NH_2-NH_2-$ or $-CH{=}CH-$.

For example, the π-electronic system of **2**-**5** can be derived from the 2 π-electron allylic moiety **1** by addition of endo- (NH groups) and exocyclic (CH_3, NH_2 and OH substituents) 2 π-

dx.doi.org/10.1021/jo302080c | J. Org. Chem. 2013, 78, 328−338

electron donors. A qualitative description of the MO diagram of **2** resulting from these moieties is given in Scheme 5, and it

Scheme 5. Qualitative π-Molecular Orbital Diagram of 2 from Combination of 1 with Two NH_2 Groups[a]

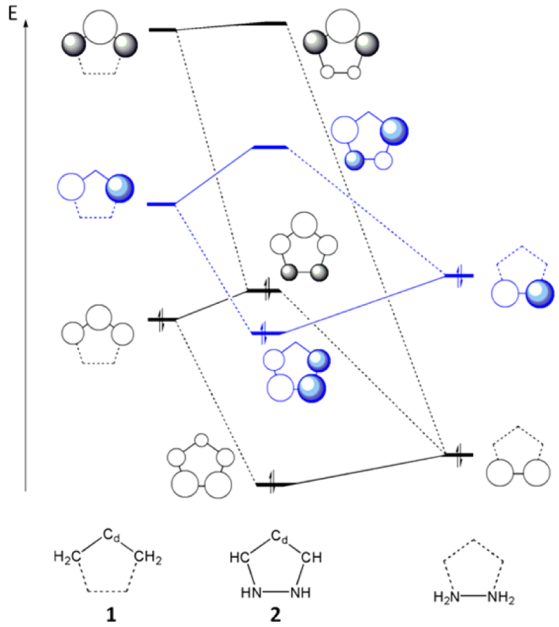

[a]The p_π orbitals are viewed from the top and represented as circles.

should be noted that the resulting MOs agree well with the π-MO's obtained at the DFT level (Figure 5). This simple decomposition of molecules into fragments provides a straightforward rationalization of their relative electronic structure. It clearly shows that as the π-donor groups increase in strength (NH_2 > OH > CH_3), the energy of the π-HOMO and the π-electronic transfer to C_d rise, in agreement both with results of the π-population at C_d and observation that compounds like **5**,[52] but not **3**,[45] can be doubly protonated. Conversely, **15** represents the association of **1** and a 3-atom/4-π-electron −CH−NH−CH− fragment that has one vacant and two occupied orbitals. Therefore π-electron density can be transferred not only from the fragment to **1**, as observed for **2**−**5**, but also from **1** to the fragment. This explains why **15** shows a lower p_π population at C_d than **2**−**5**. Finally, this description shows that the electronic structures of **5** result from a competition between the endo- and exocyclic nitrogen donor groups in transferring electron density to the CC_dC allylic moiety. Because of their similarities, both endo- and exocyclic donor groups should interact with the π-orbital of the allyl moiety to a similar degree. Thus, even though the endocyclic nitrogen atoms induce aromaticity through their delocalization into the allyl moiety, they do not enter into delocalization more efficiently than the exocyclic nitrogen atoms. This explains that exocyclic delocalization could reduce the aromaticity associated with endocyclic delocalization.[52]

This description of **1**−**5** also suggests that the replacement of the endocyclic N atoms with other 2-π-electron donor groups should lead to new stable divalent carbon compounds having similar electronic properties. This has already been shown for related oxygen derivatives.[46] Substituting the endocyclic NH groups by CH_2 groups gives **6**−**8**, which resemble **2**, **4**, and **5**, respectively. The structural proximity produces similar

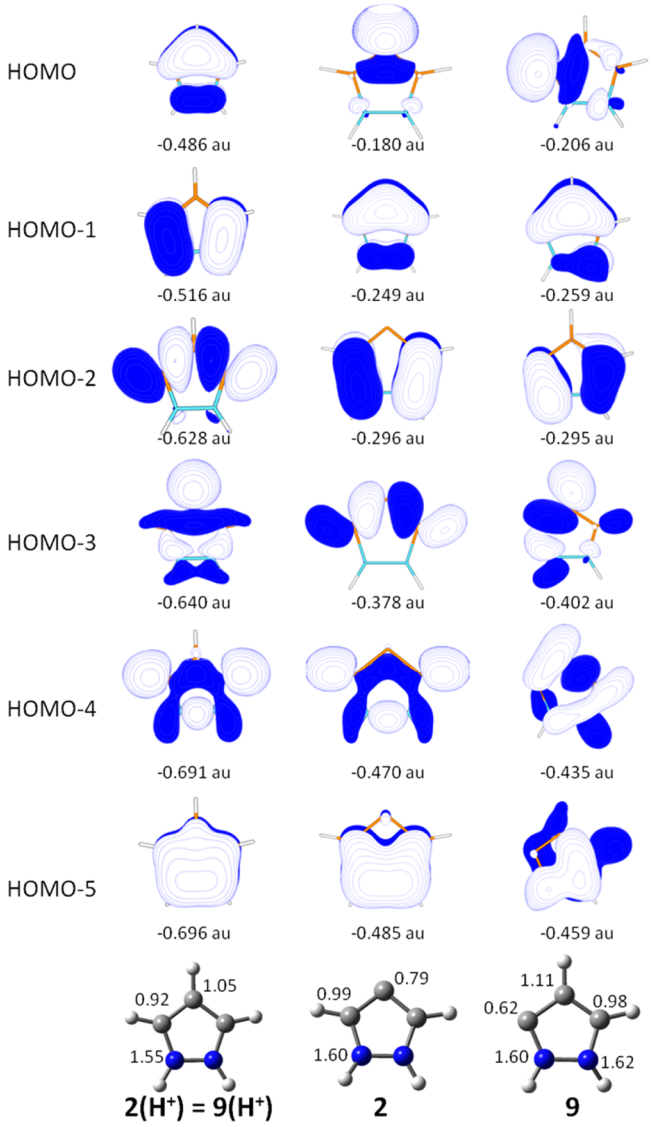

Figure 5. π-Electron population from NPA in **2**(H^+), **2**, and **9** (bottom) and their Kohn−Sham MOs (top) computed at the B3LYP/aug-cc-pVTZ level.

electronic structures as revealed by close first PA values (Figure 2). The second PA (Table S1, Supporting Information) is reduced becaue of the lower π-donating capacity of the $-CH_2-$ group, through hyperconjugation, compared to that of −NH−, but remains significant for **8**. It should be noticed that the second PA reduction is larger in **6** (compared to **2**; Δ(second PA) = −101 kJ/mol) than for **7** (compared to **4**; Δ(second PA) = −71 kJ/mol) and **8** (compared to **5**; Δ(second PA) = −45 kJ/mol), illustrating the decreasing influence of the −NH−NH− bridge in the π electronic structure in the **2**−**5** series.

Similarly, π-MOs of **11**−**13** are derived from those of **10**. Consequently, the better donor ability of −CH═CH− compared to $-CH_2-CH_2-$ explains the larger π-population at C_d in **11** compared to **13**.

A second way to deconstruct the π-MOs of **1**−**20** is to relate them to the π-MOs of **1**(H^+)−**20**(H^+). This can be achieved by substituting a "normal" sp^2 carbon atom by a C_d center having lower electronegativity. For example, both the π-MOs of **9** and **2** can be derived from those of **2**(H^+), with the site of lowered

dx.doi.org/10.1021/jo302080c | J. Org. Chem. 2013, 78, 328−338

electronegativity being at different positions in the ring. The form of the π-orbitals that are generated is comparable, but their position relative to C_d is different (Figure 5).[110]

The increase in energy that is associated with the π-AO of the less electronegative C_d relative to the π-AO of a "normal" sp^2 carbon atom means that it participates less in the occupied π-MOs. The result is that the π-population at this center is reduced by approximately the same amount for all molecules, which is in accord with the correlation observed between the π-population of **1**−**20** and **1**(H^+)−**20**(H^+) (Figure 3). To compensate, the excess π-electron density (around 0.3 e) is shared by the other atoms that comprise the π-system, as shown for **2** and **9** in Figure 5.

One noteworthy difference between the π-MOs of the molecules under study concerns the form of the π-HOMO. In most of the cases, this orbital is partially localized at the C_d center or its protonated equivalent. Furthermore, the weight at this center is larger for this MO than the other occupied MO's, as can be seen for **1** and **2** (Scheme 5 and Figure 5). This indicates that the π-basicity at the C_d center can be estimated from the $\varepsilon(\pi\text{-HOMO})$ for these molecules. However, the coefficient of the p_π atomic orbital at the C_d center is zero for **10**, **13**, **15**, and their protonated analogues, as can be seen for **10**(H^+) in Scheme 4. This means that only the HOMO-1, and not the HOMO, can be responsible for π-basicity in these molecules, which explains the weak correlation between the second PA and the $\varepsilon(\pi\text{-HOMO})$ of **1**(H^+)−**17**(H^+) that was noted previously (Figure S6, Supporting Information). Consistently, a good correlation (R^2 = 0.954) is obtained between the second PA of **1**(H^+)−**17**(H^+) and the eigenvalues of the highest π-MO partly located at the carbon atom corresponding to the protonated C_d center (Figure 6).

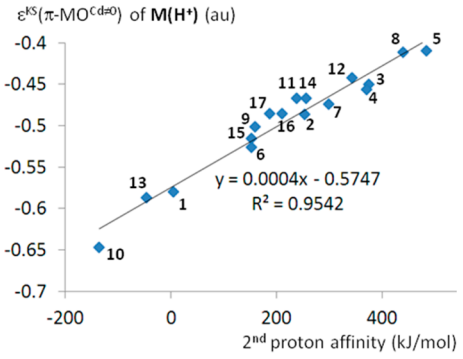

Figure 6. Plot of calculated B3LYP/aug-cc-pVTZ second proton affinities versus the Kohn−Sham eigenvalues of the π-MO with a non-zero coefficient at the carbon atom corresponding to the protonated C_d center.

Singlet−triplet Transition. It is well-known that a transition from a singlet to triplet carbene is associated with a one-electron excitation from the doubly occupied σ-lone pair at C_d (the HOMO) into the vacant p_π orbital (the LUMO; Figure 7). The π-spin density population in the vertical triplet state should therefore be a good measure of the form of the LUMO, and therefore of the π-acidity of the divalent carbon compounds.

Before analyzing the spin density in the triplet state, the vertical singlet−triplet gaps ($\Delta E^{vert}_{S\to T}$) for **1**−**17** were computed at the DFT level (Table S1, Supporting Information). The values obtained range from −20 kJ/mol for **1** to 411 kJ/mol for **11**. The $\Delta E^{vert}_{S\to T}$ values for **7** (253 kJ/mol) and **8** (253 kJ/mol) lie close to those computed for **3** (257 kJ/mol), which suggests that these compounds could be pertinent synthetic targets, as it is known that a large value indicates a compound which can normally be isolated experimentally.

Figure 8 shows that the $\Delta E^{vert}_{S\to T}$ values for **1**−**17** correlate with the energy difference between the Kohn−Sham HOMO (σ-LP) and the LUMO (correlation coefficient = 0.969). A similar correlation (R^2 = 0.945) is obtained with the LUMO of the protonated analogues. This indicates that the energy decrease of the LUMO upon protonation is broadly similar in compounds **1**−**17**. This result is consistent with the general energy decrease of the p_π orbital at C_d center upon protonation (vide infra).

DFT calculations, which were made to evaluate the spin density population that results from the singlet−triplet transition (Figure 7 and Table S1, Supporting Information), show that the expected spin density is found in the plane of the molecule (σ-spin density) and perpendicular to it (π-spin density) in all cases. For NHCs, the π-spin density is mostly located at C_d (**11** in Figure 7). However, the vertical triplet state of **1**−**8** (**2** in Figure 7) shows no π-spin density in the p_π orbital at C_d; the promoted electron in the triplet state is delocalized around the π-system but absent from C_d. This result reflects the different form of the LUMO in **1**(H^+) and **10**(H^+) (Scheme 4). For **1**(H^+), the LUMO is Φ_2, which is located in the terminal carbon, while for **10**(H^+) it is Φ_3, which is located mainly on the central carbon. We have shown above that **1** and **1**(H^+) have similar π-MOs and that **2**−**8** can be obtained from **1** after interaction with doubly occupied π-MOs (Scheme 5). Therefore, the LUMOs of **1**−**8** are similar, and this explains the π-spin density at C_d and the low π-acidity of these divalent carbon compounds. Finally, the parallels in the occupied π-MOs of **2** and **9** (vide infra) are also found in the π-LUMO, where the π-spin density analysis shows similar values for the different atoms of the ring (Figure 7).

■ CONCLUSION

The family of *N*-heterocyclic carbenes and related compounds contains an increasing number of members that possess a wide range of electronic properties. In this work, we have used computational methods to rationalize the σ- and π-electronic properties of these derivatives. The σ-basicity, which reflects the energy of the σ-LP, is influenced by the charge of the divalent carbon species, the identity of the atoms neighboring C_d, and the nature of the *trans* X_α−Y_β bond. Calculation of π-population data sheds new light on the nature of these divalent compounds and brings out trends and similarities. The divalent carbon compounds treated result from deprotonation of π-delocalized or aromatic structures that are based on allyl cation, imidazolium, pyrazolium, pyridinium, or phenyl backbones, and the deprotonation creates a formal localized negative charge that is associated with the σ-lone pair at the C_d center. For neutral compounds, the electrons of the π-system can either neutralize this negative charge, which is the case if the π-population is low at the C_d center (NHCs), or does not, if the positive charge is mainly delocalized over the ring (MICs). This leads to a continuum of structures that range from classical NHCs to mesoionic "carbenes". Monoanionic ligands are comparable to mesoions in terms of π-population because the negative charge on the C_d center is not quenched. The divalent carbon compounds therefore form a nondiscontinuous family

dx.doi.org/10.1021/jo302080c | J. Org. Chem. 2013, 78, 328−338

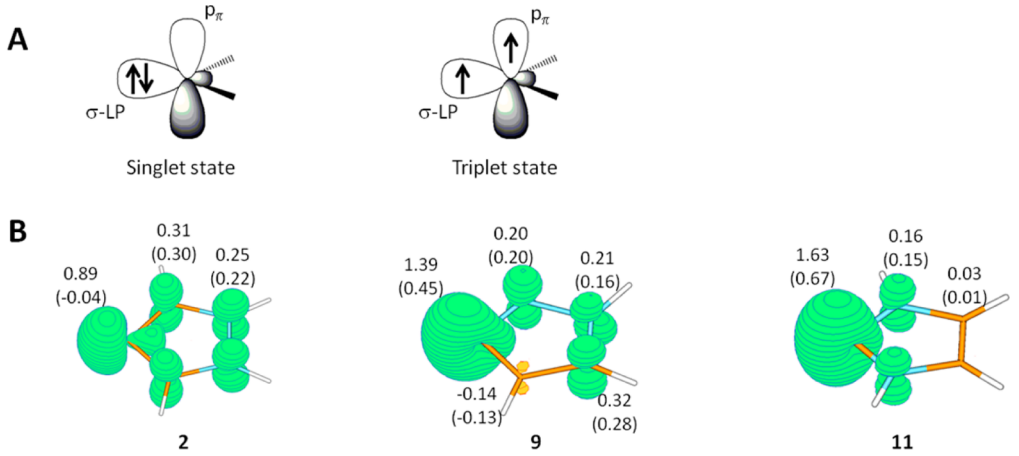

Figure 7. (A) Electronic configurations of carbenes. (B) B3LYP/aug-cc-pVTZ spin density (isosurface at 0.02 au) and total NBO spin density population ($\alpha-\beta$) (π-spin density population in parentheses) for vertical triplet states of **2**, **9**, and **11**.

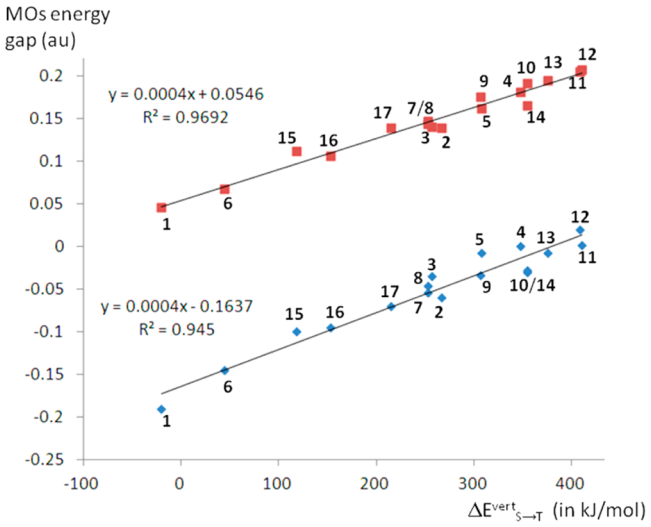

Figure 8. Plot of vertical singlet−triplet energy gap versus the energy difference between σ-LP of **1**−**17** and their LUMO (red) or the LUMO of their protonated analogues (blue).

with respect to their electronic properties, even if it is not possible to represent them all by the same sort of Lewis representations. Unlike the σ-system, there are no structural criteria that predict the nature of the π-system. However, trends observed in the distribution of π-electron density can be explained by a qualitative description of the π-MOs, which can be related to those of the protonated analogues by simply increasing the energy of the p_π orbital at the divalent carbon atom beyond that of a normal sp^2 carbon. The π-MOs can be used to explain both the π-acidity and π-basicity of these compounds and why exocyclic delocalization can reduce the aromaticity associated with endocyclic delocalization in the mesoionic carbene **5**.

We hope that the reported results will contribute positively to a deeper understanding of these intriguing compounds. Further work is in progress to rationalize the electronic structure of these divalent carbon compounds with respect to their σ-donor and π-acceptor capabilities toward transition metal fragments.

COMPUTATIONAL METHODS

Geometry optimizations of all compounds have been performed without constraints (except where noted) at the B3LYP[111,112] level with the Gaussian09 program.[113] All atoms were described with the correlation consistent aug-cc-pVTZ basis set.[114,115] A vibrational analysis of **1**−**20** and their protonated counterpart **1**(H^+)-**20**(H^+), performed after optimization, confirms that these molecules represent minima on the PES except for **1** and **6**, which possess one imaginary frequency. Geometry optimization of **1** and **6** without constraints leads to the parent allene **1′** with linear CCC moiety and orthogonal configuration of the CH_2 groups and to nonplanar "bent allene" **6′**[116] with H−C−C−C dihedral angles of 158.0°, respectively (Scheme 6).

Scheme 6. Structures of 1′ and 6′

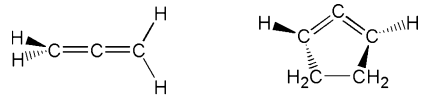

1′ **6′**

Constraining the planar geometry during the optimization process results in **1** and **6**, which are located 321 and 15 kJ/mol higher in energy than **1′** and **6′**, respectively. The $R_2C-C_d-CR_2$ planar arrangement in **1** and **6** around the C_d divalent carbon parallels the one observed in **2**, allowing straightforward comparison (vide supra).

Natural bond orbital (NBO) analysis,[117−119] performed at the same level of calculation, gives the atomic charges through natural population analysis (NPA). Second-order perturbation theory is used to estimate the energy associated with two-electron donor−acceptor orbital interactions. The π-electron population of closed shell systems is obtained from the occupancy of the p_π natural atomic orbitals (NAO). For open-shell triplet states, the spin density or the π-spin density populations are obtained from the difference between α-spin and β-spin NPA atomic charges or p_π NAO occupancies, respectively.

Energetic data discussed in the text are derived from electronic energies. Similar trends and correlations are obtained from values including zero-point and thermal corrections (Table S2, Supporting Information).

Hückel formalism has been used to drawn qualitative explanations, and Hückel molecular orbital diagram were obtained with the Hückel simple program.[120]

ASSOCIATED CONTENT

Supporting Information

Optimized geometries (Figures S1 and S2); NPA-calculated π-population and atomic charges (Figures S3 and S4); plots of

dx.doi.org/10.1021/jo302080c | J. Org. Chem. 2013, 78, 328−338

calculated NPA π-population versus atomic charge at C_d (Figure S5) and of calculated second PA versus the NPA π-population or the Kohn−Sham eigenvalues of the HOMO (Figure S6); π-electron population and Kohn−Sham MOs of **9** and its planar constrained geometry **9p** (Figure S7); computed electronic and chemical properties of **1**−**20** (Tables S1 and S2); absolute energies (Tables S3−S5) and atom coordinates (Table S6) of all compounds. This material is available free of charge via the Internet at http://pubs.acs.org.

AUTHOR INFORMATION

Corresponding Author

*Tel: +33 (0)1 69 33 48 34. Fax: +33 (0)1 69 33 48 03. E-mail: gilles.frison@polytechnique.org.

Notes

The authors declare no competing financial interest.

ACKNOWLEDGMENTS

This work was granted access to the HPC resources of CINES under the allocation 2012-c2012086894 made by GENCI (Grand Equipement National de Calcul Intensif). We thank Dr. Duncan Carmichael for helpful comments and improvements on the manuscript.

REFERENCES

(1) Igau, A.; Grützmacher, H.; Baceiredo, A.; Bertrand, G. *J. Am. Chem. Soc.* **1988**, *110*, 6463−6466.
(2) Igau, A.; Baceiredo, A.; Trinquier, G.; Bertrand, G. *Angew. Chem., Int. Ed. Engl.* **1989**, *28*, 621−622.
(3) Martin, D.; Melaimi, M.; Soleilhavoup, M.; Bertrand, G. *Organometallics* **2011**, *30*, 5304−5313.
(4) Arduengo, A. J., III; Harlow, R. L.; Kline, M. *J. Am. Chem. Soc.* **1991**, *113*, 361−363.
(5) Bourissou, D.; Guerret, O.; Gabbaï, F. P.; Bertrand, G. *Chem. Rev.* **2000**, *100*, 39−91.
(6) Hahn, F. E.; Jahnke, M. C. *Angew. Chem., Int. Ed.* **2008**, *47*, 3122−3172.
(7) Öfele, K.; Tosh, E.; Taubmann, C.; Herrmann, W. A. *Chem. Rev.* **2009**, *109*, 3408−3444.
(8) Ingleson, M. J.; Layfield, R. A. *Chem. Commun.* **2012**, *48*, 3579−3589.
(9) Wang, Y.; Robinson, G. H. *Inorg. Chem.* **2011**, *50*, 12326−12337.
(10) Al-Rafia, S. M. I.; Malcolm, A. C.; Liew, S. K.; Ferguson, M. J.; Rivard, E. *J. Am. Chem. Soc.* **2011**, *133*, 777−779.
(11) Curran, D. P.; Solovyev, A.; Makhlouf Brahmi, M.; Fensterbank, L.; Malacria, M.; Lacôte, E. *Angew. Chem., Int. Ed.* **2011**, *50*, 10294−10317.
(12) Wang, Y.; Robinson, G. H. *Dalton Trans.* **2012**, *41*, 337−345.
(13) Kinjo, R.; Donnadieu, B.; Celik, M. A.; Frenking, G.; Bertrand, G. *Science* **2011**, *333*, 610−613.
(14) Martin, D.; Soleilhavoup, M.; Bertrand, G. *Chem. Sci.* **2011**, *2*, 389−399.
(15) Herrmann, W. A. *Angew. Chem., Int. Ed.* **2002**, *41*, 1290−1309.
(16) Schuster, O.; Yang, L.; Raubenheimer, H. G.; Albrecht, M. *Chem. Rev.* **2009**, *109*, 3445−3478.
(17) Nolan, S. P. *Acc. Chem. Res.* **2011**, *44*, 91−100.
(18) Correa, A.; Nolan, S. P.; Cavallo, L. *Top. Curr. Chem.* **2011**, *302*, 131−155.
(19) Valente, C.; Calimsiz, S.; Hoi, K. H.; Mallik, D.; Sayah, M.; Organ, M. G. *Angew. Chem., Int. Ed.* **2012**, *51*, 3314−3332.
(20) Enders, D.; Niemeier, O.; Henseler, A. *Chem. Rev.* **2007**, *107*, 5606−5655.
(21) Marion, N.; Diez-Gonzalez, S.; Nolan, S. P. *Angew. Chem., Int. Ed.* **2007**, *46*, 2988−3000.
(22) Biju, A. T.; Kuhl, N.; Glorius, F. *Acc. Chem. Res.* **2011**, *44*, 1182−1195.
(23) Bugaut, X.; Glorius, F. *Chem. Soc. Rev.* **2012**, *41*, 3511−3522.
(24) Diez-Gonzalez, S.; Nolan, S. P. *Coord. Chem. Rev.* **2007**, *251*, 874−883.
(25) Vignolle, J.; Cattoën, X.; Bourissou, D. *Chem. Rev.* **2009**, *109*, 3333−3384.
(26) Melaimi, M.; Soleilhavoup, M.; Bertrand, G. *Angew. Chem., Int. Ed.* **2010**, *49*, 8810−8849.
(27) Dröge, T.; Glorius, F. *Angew. Chem., Int. Ed.* **2010**, *49*, 6940−6952.
(28) Moerdyk, J. P.; Bielawski, C. W. *Nat. Chem.* **2012**, *4*, 275−280.
(29) Trnka, T. M.; Grubbs, R. H. *Acc. Chem. Res.* **2001**, *34*, 18−29.
(30) Kantchev, E. A. B.; O'Brien, C. J.; Organ, M. G. *Angew. Chem., Int. Ed.* **2007**, *46*, 2768−2813.
(31) Arnold, P. L.; Pearson, S. *Coord. Chem. Rev.* **2007**, *251*, 596−609.
(32) Raubenheimer, H. G.; Cronje, S. *Dalton Trans.* **2008**, 1265−1272.
(33) Albrecht, M. *Chem. Commun.* **2008**, 3601−3610.
(34) Tonner, R.; Öxler, F.; Neumüller, B.; Petz, W.; Frenking, G. *Angew. Chem., Int. Ed.* **2006**, *45*, 8038−8042.
(35) Tonner, R.; Frenking, G. *Angew. Chem., Int. Ed.* **2007**, *46*, 8695−8698.
(36) Emanuel, C. J.; Shevlin, P. B. *J. Am. Chem. Soc.* **1994**, *116*, 5991−5992.
(37) Pan, W.; Shevlin, P. B. *J. Am. Chem. Soc.* **1997**, *119*, 5091−5094.
(38) Schöneboom, J. C.; Groetsch, S.; Christl, M.; Engels, B. *Chem.—Eur. J.* **2003**, *9*, 4641−4649.
(39) Musch, P. W.; Scheidel, D.; Engels, B. *J. Phys. Chem. A* **2003**, *107*, 11223−11230.
(40) Schuster, O.; Raubenheimer, H. G. *Inorg. Chem.* **2006**, *45*, 7997−7999.
(41) Esterhuysen, C.; Frenking, G. *Chem.—Eur. J.* **2011**, *17*, 9944−9956.
(42) Guha, A. K.; Phukan, A. K. *Chem.—Eur. J.* **2012**, *18*, 4419−4425.
(43) Araki, S.; Wanibe, Y.; Uno, F.; Morikawa, A.; Yamamoto, K.; Chiba, K.; Butsugan, Y. *Chem. Ber.* **1994**, *126*, 1149−1155.
(44) Aldeco-Perez, E.; Rosenthal, A. J.; Donnadieu, B.; Parameswaran, P.; Frenking, G.; Bertrand, G. *Science* **2009**, *326*, 556−559.
(45) Han, Y.; Huynh, H. V. *Dalton Trans.* **2011**, *40*, 2141−2147.
(46) Iglesias, M.; Albrecht, M. *Dalton Trans.* **2010**, *39*, 5213−5215.
(47) The allene description of the electronic structure of **E** (**E9** type) is not only formal, as shown by Tuononen et al. (ref 48), but also greatly misleading: in such a description, the location of the electrons is unclear. The planarity of the molecule associated with two C═C bonds should induce four π-electrons along the same axis, whereas the allene presentation refers to two orthogonal π systems, one being in the σ-plane of the molecule.
(48) Hänninen, M. M.; Peuronen, A.; Tuononen, H. M. *Chem.—Eur. J.* **2009**, *15*, 7287−7291.
(49) Lavallo, V.; Dyker, C. A.; Donnadieu, B.; Bertrand, G. *Angew. Chem., Int. Ed.* **2008**, *47*, 5411−5414.
(50) Christl, M.; Engels, B. *Angew. Chem., Int. Ed.* **2009**, *48*, 1538−1539.
(51) Lavallo, V.; Dyker, C. A.; Donnadieu, B.; Bertrand, G. *Angew. Chem., Int. Ed.* **2009**, *48*, 1540−1542.
(52) Fernandez, I.; Dyker, C. A.; DeHope, A.; Donnadieu, B.; Frenking, G.; Bertrand, G. *J. Am. Chem. Soc.* **2009**, *131*, 11875−11881.
(53) Magill, A. M.; Cavell, K. J.; Yates, B. F. *J. Am. Chem. Soc.* **2004**, *126*, 8717−8724.
(54) Nyulaszi, L.; Veszpremi, T.; Forro, A. *Phys. Chem. Chem. Phys.* **2000**, *2*, 3127−3129.
(55) Frison, G.; Sevin, A. *J. Chem. Soc., Perkin Trans. 2* **2002**, 1692−1697.
(56) Kausamo, A.; Tuononen, H. M.; Krahulic, K. E.; Roesler, R. *Inorg. Chem.* **2008**, *47*, 1145−1154.
(57) Maji, B.; Breugst, M.; Mayr, H. *Angew. Chem., Int. Ed.* **2011**, *50*, 6915−6919.

(58) Schneider, S. K.; Julius, G. R.; Loschen, C.; Raubenheimer, H. G.; Frenking, G.; Herrmann, W. A. *Dalton Trans.* **2006**, 1226−1233.
(59) Alcarazo, M.; Stork, T.; Anoop, A.; Thiel, W.; Fürstner, A. *Angew. Chem., Int. Ed.* **2010**, *49*, 2542−2546.
(60) Boehme, C.; Frenking, G. *Organometallics* **1998**, *17*, 5801−5809.
(61) Lein, M.; Szabo, A.; Kovacs, A.; Frenking, G. *Faraday Discuss.* **2003**, *124*, 365−378.
(62) Nemcsok, D.; Wichmann, K.; Frenking, G. *Organometallics* **2004**, *23*, 3640−3646.
(63) Schneider, S. K.; Roembke, P.; Julius, G. R.; Loschen, C.; Raubenheimer, H. G.; Frenking, G.; Herrmann, W. A. *Eur. J. Inorg. Chem.* **2005**, 2973−2977.
(64) Tonner, R.; Heydenrych, G.; Frenking, G. *Chem. Asian J.* **2007**, *2*, 1555−1567.
(65) Tonner, R.; Frenking, G. *Organometallics* **2009**, *28*, 3901−3905.
(66) Chianese, A. R.; Li, X.; Janzen, M. C.; Faller, J. W.; Crabtree, R. H. *Organometallics* **2003**, *22*, 1663−1667.
(67) Termaten, A. T.; Schakel, M.; Ehlers, A. W.; Lutz, M.; Spek, A. L.; Lammertsma, K. *Chem.—Eur. J.* **2003**, *9*, 3577−3582.
(68) Comas-Vives, A.; Harvey, J. N. *Eur. J. Inorg. Chem.* **2011**, *32*, 5025−5035.
(69) Srebro, M.; Michalak, A. *Inorg. Chem.* **2009**, *48*, 5361−5369.
(70) Antonova, N. S.; Carbo, J. J.; Poblet, J. M. *Organometallics* **2009**, *28*, 4283−4287.
(71) Deubel, D. V. *Organometallics* **2002**, *21*, 4303−4305.
(72) Mercs, L.; Labat, G.; Neels, A.; Ehlers, A.; Albrecht, M. *Organometallics* **2006**, *25*, 5648−5656.
(73) Penka, E. F.; Schläpfer, C. W.; Atanasov, M.; Albrecht, M.; Daul, C. *J. Organomet. Chem.* **2007**, *692*, 5709−5716.
(74) Hu, X.; Castro-Rodriguez, I.; Olsen, K.; Meyer, K. *Organometallics* **2004**, *23*, 755−764.
(75) Radius, U.; Bickelhaupt, F. M. *Organometallics* **2008**, *27*, 3410−3414.
(76) Radius, U.; Bickelhaupt, F. M. *Coord. Chem. Rev.* **2009**, *253*, 678−686.
(77) Wolf, S.; Plenio, H. *J. Organomet. Chem.* **2009**, *694*, 1487−1492.
(78) Kelly, R. A., III; Clavier, H.; Guidice, S.; Scott, N. M.; Stevens, E. D.; Bordner, J.; Samardjiev, I.; Hoff, C. D.; Cavallo, L.; Nolan, S. P. *Organometallics* **2008**, *27*, 202−210.
(79) Jacobsen, H.; Correa, A.; Costabile, C.; Cavallo, L. *J. Organomet. Chem.* **2006**, *691*, 4350−4358.
(80) Fantasia, S.; Petersen, J. L.; Jacobsen, H.; Cavallo, L.; Nolan, S. P. *Organometallics* **2007**, *26*, 5880−5889.
(81) Jacobsen, H.; Correa, A.; Poater, A.; Costabile, C.; Cavallo, L. *Coord. Chem. Rev.* **2009**, *253*, 687−703.
(82) Gusev, D. G. *Organometallics* **2009**, *28*, 763−770.
(83) Gusev, D. G. *Organometallics* **2009**, *28*, 6458−6461.
(84) Braun, M.; Frank, W.; Ganter, C. *Organometallics* **2012**, *31*, 1927−1934.
(85) Credendino, R.; Falivene, L.; Cavallo, L. *J. Am. Chem. Soc.* **2012**, *134*, 8127−8135.
(86) Bernhammer, J. C.; Huynh, H. V. *Dalton Trans.* **2012**, *41*, 8600−8608.
(87) Hobbs, M. G.; Knapp, C. J.; Welsh, P. T.; Borau-Garcia, J.; Ziegler, T.; Roesler, R. *Chem.—Eur. J.* **2010**, *16*, 14520−14533.
(88) Wang, Y.; Xie, Y.; Abraham, M. Y.; Wei, P.; Schaefer, H. F., III; Schleyer, P. V. R.; Robinson, G. H. *J. Am. Chem. Soc.* **2010**, *132*, 14370−14372.
(89) Wang, Y.; Xie, Y.; Abraham, M. Y.; Wei, P.; Schaefer, H. F., III; Schleyer, P. V. R.; Robinson, G. H. *Organometallics* **2011**, *30*, 1303−1306.
(90) Jana, A.; Azhakar, R.; Tavcar, G.; Roesky, H. W.; Objartel, I.; Stalke, D. *Eur. J. Inorg. Chem.* **2011**, 3686−3689.
(91) Yao, Q.; Zabawa, M.; Woo, J.; Zheng, C. *J. Am. Chem. Soc.* **2007**, *129*, 3088−3089.
(92) Briggs, P. M.; Young, V. G., Jr; Wigley, D. E. *Chem. Commun.* **1997**, 791−792.
(93) Oulié, P.; Nebra, N.; Saffon, N.; Maron, L.; Martin-Vaca, B.; Bourissou, D. *J. Am. Chem. Soc.* **2009**, *131*, 3493−3498.
(94) Tafipolsky, M.; Scherer, W.; Öfele, K.; Artus, G.; Pedersen, B.; Herrmann, W. A.; McGrady, G. S. *J. Am. Chem. Soc.* **2002**, *124*, 5865−5880.
(95) Heinemann, C.; Müller, T.; Apeloig, Y.; Schwarz, H. *J. Am. Chem. Soc.* **1996**, *118*, 2023−2038.
(96) Tonner, R.; Heydenrych, G.; Frenking, G. *ChemPhysChem* **2008**, *9*, 1474−1481.
(97) Klein, S.; Tonner, R.; Frenking, G. *Chem.—Eur. J.* **2010**, *16*, 10160−10170.
(98) Bent, H. A. *Can. J. Chem.* **1960**, *38*, 1235−1237.
(99) Huynh, H. V.; Han, Y.; Jothibasu, R.; Yang, J. A. *Organometallics* **2009**, *28*, 5395−5404.
(100) Mayr, M.; Wurst, K.; Ongania, K.; Buchmeiser, M. R. *Chem.—Eur. J.* **2004**, *10*, 1256−1266.
(101) Iglesias, M.; Beetstra, D. J.; Stasch, A.; Horton, P. N.; Hursthouse, M. B.; Coles, S. J.; Cavell, K. J.; Dervisi, A.; Fallis, I. A. *Organometallics* **2007**, *26*, 4800−4809.
(102) Iglesias, M.; Beetstra, D. J.; Knight, J. C.; Ooi, L.; Stasch, A.; Coles, S.; Male, L.; Hursthouse, M. B.; Cavell, K. J.; Dervisi, A.; Fallis, I. A. *Organometallics* **2008**, *27*, 3279−3289.
(103) Scarborough, C. C.; Guzei, I. A.; Stahl, S. S. *Dalton Trans.* **2009**, 2284−2286.
(104) Frison, G.; Sevin, A. *J. Phys. Chem. A* **1999**, *103*, 10998−11003.
(105) In that sense, the use of the term "mesoionic carbene" is formally not always fully adequate as IUPAC indicates that both the positive and the negative charge are delocalized in a mesoionic compound. We, however, recommend still using it due to the absence of a proper denomination.
(106) The π-HOMO is defined as being the highest occupied molecular orbital with π-symmetry. This is the HOMO-1 for **1**−**20** and the HOMO for $\mathbf{1}(\mathbf{H}^+)$−$\mathbf{20}(\mathbf{H}^+)$ except for $\mathbf{18}^{a}(\mathbf{H}^+)$ and $\mathbf{18}^{n}(\mathbf{H}^+)$, where the π-HOMO is the HOMO-1.
(107) Gillespie, R. J. *J. Chem. Educ.* **1970**, *47*, 18−23.
(108) Hückel, E. *Z. Phys.* **1931**, *70*, 204−286.
(109) Streitwieser, A. *Molecular Orbital Theory for Organic Chemists*; Wiley: New York, 1961.
(110) It should be noted that the nonplanarity of **9** does not change the π-density significantly. Indeed, computing **9** in a planar constrained geometry leads to **9p**, which is located 0.6 kJ/mol higher in energy and shows only a small qualitative difference in its π distribution compared to **9** (Figure S7, Supporting Information).
(111) Becke, A. D. *J. Chem. Phys.* **1993**, *98*, 5648−5652.
(112) Lee, C. T.; Yang, W. T.; Parr, R. G. *Phys. Rev. B* **1988**, *37*, 785−789.
(113) Frisch, M. J.; Trucks, G. W.; Schlegel, H. B.; Scuseria, G. E.; Robb, M. A.; Cheeseman, J. R.; Scalmani, G.; Barone, V.; Mennucci, B.; Petersson, G. A.; Nakatsuji, H.; Caricato, M.; Li, X.; Hratchian, H. P.; Izmaylov, A. F.; Bloino, J.; Zheng, G.; Sonnenberg, J. L.; Hada, M.; Ehara, M.; Toyota, K.; Fukuda, R.; Hasegawa, J.; Ishida, M.; Nakajima, T.; Honda, Y.; Kitao, O.; Nakai, H.; Vreven, T.; Montgomery, J. A., Jr; Peralta, J. E.; Ogliaro, F.; Bearpark, M.; Heyd, J. J.; Brothers, E.; Kudin, K. N.; Staroverov, V. N.; Keith, T.; Kobayashi, R.; Normand, J.; Raghavachari, K.; Rendell, A.; Burant, J. C.; Iyengar, S. S.; Tomasi, J.; Cossi, M.; Rega, N.; Millam, J. M.; Klene, M.; Knox, J. E.; Cross, J. B.; Bakken, V.; Adamo, C.; Jaramillo, J.; Gomperts, R.; Stratmann, R. E.; Yazyev, O.; Austin, A. J.; Cammi, R.; Pomelli, C.; Ochterski, J. W.; Martin, R. L.; Morokuma, K.; Zakrzewski, V. G.; Voth, G. A.; Salvador, P.; Dannenberg, J. J.; Dapprich, S.; Daniels, A. D.; Farkas, O.; Foresman, J. B.; Ortiz, J. V.; Cioslowski, J.; Fox, D. J. Gaussian 09, revision B.01, Gaussian, Inc., Wallingford, CT, 2010.
(114) Dunning, T. H. *J. Chem. Phys.* **1989**, *90*, 1007−1023.
(115) Woon, D. E.; Dunning, T. H. *J. Chem. Phys.* **1993**, *98*, 1358−1371.
(116) Daoust, K. J.; Hernandez, S. M.; Konrad, K. M.; Mackie, I. D.; Winstanley, J., Jr; Johnson, R. P. *J. Org. Chem.* **2006**, *71*, 5708−5714.
(117) Reed, A. E.; Weinhold, F. *J. Chem. Phys.* **1985**, *83*, 1736−1740.

(118) Reed, A. E.; Weinstock, R. B.; Weinhold, F. *J. Chem. Phys.* **1985**, *83*, 735−746.
(119) Reed, A. E.; Curtis, L. A.; Weinhold, F. *Chem. Rev.* **1988**, *88*, 899−926.
(120) Magna, J.-Y. Hückel simple version 4.0, 1998; http://jymagna.com.